https://doi.org/10.5194/essd-2025-771
Preprint. Discussion started: 25 February 2026

Open Access Earth System Science Data Discussions

Development of a global in-situ daily temperature dataset preferentially for 0000-2400 UTC from 1981-2024

Su Yang[1], Panmao Zhai[2], Xuebin Zhang[3], Zijiang Zhou[1*]

[1]National Meteorological Information Centre, Beijing, China
[2]State Key Laboratory of Severe Weather, Chinese Academy of Meteorolgical Sciences,
[3]Pacific Climate Impacts Consortium, University of Victoria, Victoria BC, Canada.
Correspondence to: Su Yang(yangsol.nice@outlook.com); Zijiang Zhou(zzj@cma.gov.cn)

1. Abstract

Large amounts of sub-daily temperature data are shared globally through the Global Telecommunication System (GTS) in near-real time and through international data exchanges. However, converting these data into a global daily temperature dataset with a uniform definition—especially for daily maximum (Tmax) and minimum (Tmin) temperatures—has proven challenging due to the independent observation schedules across the world. To address this issue, we developed a new method that decomposes sub-daily Tmax and Tmin records from the Integrated Surface Database (ISD) into finer intervals, subsequently reaggregating them into daily Tmax and Tmin based on prospective dateline. This new method increased the global daily Tmax and Tmin counts by 64% and 45%, respectively, compared to the original method, which relied on either two consecutive Tmax/Tmin records over 12 hours or a single Tmax/Tmin record over 24 hours. The Global Land Base Dataset-First Estimate Daily Data (GLBD-FED) was established for the period from 1981 to 2024, following corrections for misrecorded Tmax and Tmin and quality control. GLBD-FED includes daily maximum (Tmax), average

https://doi.org/10.5194/essd-2025-771
Preprint. Discussion started: 25 February 2026

(Tave), and minimum temperature (Tmin) from approximately 17,000 global sites, with daily data amounts reaching about 10,000 entries per day in the current decade. When compared to the Global Summary of the Day (GSOD) dataset, GLBD-FED exhibits more temperate performance over the last 40 years, showing a slightly lower daily Tmax (around -0.3°C) and a higher daily Tmin (around +0.3°C), with a nearly identical daily Tave (approximately +0.1°C). GLBD-FED identifies records that could or almost could represent the highest or lowest temperature in the 24-hour period as daily Tmax or Tmin, while GSOD selects the highest or lowest records within the 24 hours. This variance in definitions, combined with different preferences for meteorological and airport report sources, contributes to these observed biases. The database and associated data can be found at https://doi.org/10.5281/zenodo.17895292 (Su et al., 2025).

2. Introduction

Global in-situ daily temperature measurements are essential data resources for assessing living environments, agricultural systems, and climate-related studies(IPCC, 2021). They play critical roles in monitoring extreme weather, detecting climate change, and validating satellite observations and reanalysis products.(Beck et al., 2017, 2019; Dietzsch et al., 2017; Harris et al., 2014, 2020; Jones and Hulme, 1996; Jones and Moberg, 2003; Mitchell and Jones, 2005; New et al., 1999, 2000; Schneider et al., 2018).

Multiple research institutions and National Hydrometeorological Services (NMHSs) have developed global observational datasets (Adler RF, Huffman GJ, Chang A, Ferraro R, Xie P, Janowiak J, Rudolf B, Schneider U, Curtis S, Bolvin D, Gruber A, Susskind J, 2003; Daly, 2002; Harris et al., 2014; Hulme, 1991, 1992; Janowiak et al., 1998; Kamiguchi et al., 2010; Klein Tank et al., 2002; Menne et al., 2012; Rudolf, 1993; Schamm et al., 2014; Schneider, 1993; Xie et al., 2007; Yatagai et al., 2012). Recent advancements have progressed from monthly aggregates to daily and sub-daily products (Blenkinsop et al., 2018; Schamm et al., 2014; Westra1 et al., 2014). The Global Summary of the Day (GSOD)

https://doi.org/10.5194/essd-2025-771
Preprint. Discussion started: 25 February 2026

released by the National Centers for Environmental Information (NCEI, 2017) is one of the most widely-used global quasi-real-time daily products. It relies on the Integrated Surface Database (ISD) published by NCEI (Smith et al., 2011) as its main data source utilizing the hourly average temperature (Tave), 12 and 24-hours (h) cumulative maximum (Tmax) and minimum temperature (Tmin) to creates daily Tave, Tmax, Tmin values.

Similar to the processing of precipitation data, temperature records also include cumulative data for specific durations, such as Tmax/Tmin over 12 and 24 hours, which are recorded on a non-uniform observation schedule worldwide (WMO, 2015). Consequently, global daily temperature data, particularly for Tmax and Tmin, face temporal representation issues akin to those encountered with precipitation data. To address this, GSOD defines the maximum and minimum records occurring within a day as the daily Tmax and Tmin, respectively. While this method generally performs well, it presents challenges due to the non-standardized and unstable nature of global observations.

This study aims to produce a global daily dataset representing the maximum, minimum, and average temperatures over a 24-hour period, effectively encapsulating one day. To achieve this, we developed new algorithms for optimally utilizing the irregularly timed sub-daily measurements in the ISD and harmonizing them under consistent temporal references. The data sources and methodology are detailed in Sections 3 and 4, followed by a comparative evaluation against the daily temperature dataset defined by different methods (GSOD) in Section 5. Finally, conclusions from this study are presented in Section 6.

3. Data Sources

3.1. Near-real time sub-daily meteorological measurements

Hourly surface temperature observations spanning 1981-2024 were compiled through the

https://doi.org/10.5194/essd-2025-771
Preprint. Discussion started: 25 February 2026

Integrated Surface Database (ISD), a global database that consists of hourly and synoptic surface observations compiled from numerous sources into a single common ASCII format and common data model(Smith et al., 2011).

The ISD-derived temperature parameters encompass five temporal resolution components: hourly mean temperature (Tave), 24-hour maxima and minima (Tmax-24h and Tmin-24h), and 12-hour maxima and minima (Tmax-12h and Tmin-12h). Fig.1 illustrates their global temporal distributions from 2011 to 2024, with panels a-c corresponding to Tave, Tmax-24h/Tmin-24h, and Tmax-12h/Tmin-12h, respectively. Analysis reveals two dominant regimes for Tave observations with 6-hour cadences: 0000/0600/1200/1800 UTC (approximately 95×10^6 records per hour) and 0300/0900/1500/2100 UTC (approximately 70×10^6 records per hour). This four-peak temporal distribution supports the computational efficiency of deriving daily Tave through quad-hourly sampling at 6-hour intervals, offering an optimized solution for global temperature averaging.

Tmax/Tmin-24h (Fig.1 panel b) show significantly fewer records compared to Tave. Eight synoptic times (0000/0300/0600/0900/1200/1500/1800/2100 UTC) exhibit uniform data densities for Tmax and Tmin-24h, with peaks at 0000 and 0600 UTC (approximately 27×10^6 records per hour) containing three times the volume of adjacent times (around 9×10^6 records per hour). This suggests a potential date shift or inhomogeneity between daily Tmax and Tmin records from different regions if Tmax and Tmin-24h are treated as global daily data directly. In contrast, Tmax/Tmin-12h do not exhibit a similar distribution to the 24-hour records (Fig.1 panel c), being predominantly clustered at 0000/0600/1200/1800 UTC with 6 to 26×10^6 records per hour.

In summary, Tmax and Tmin display weaker temporal regularity compared to Tave. Moreover, Tmax and Tmin do not always appear in pairs as expected, indicating that date shifts and inhomogeneities may not only exist between regions but also between the raw

https://doi.org/10.5194/essd-2025-771
Preprint. Discussion started: 25 February 2026

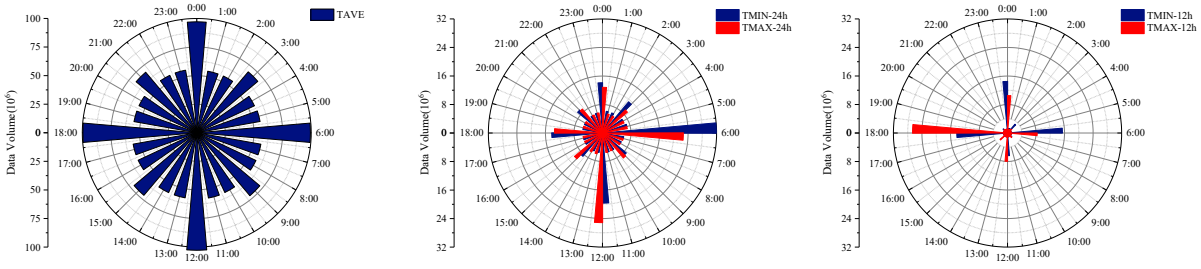

Figure 1 The distribution of sub-daily temperature data amounts at each o'clock during 2011-2024

3.2. GSOD in-situ daily data

The Global Surface Summary of the Day (GSOD; accessible at https://data.noaa.gov/dataset/dataset/groups/global-surface-summary-of-the-day-gsod), maintained by the U.S. National Centers for Environmental Information (NCEI), generates daily meteorological summaries from over 9,000 global weather stations. Derived through systematic processing of the ISD, this product provides continuous records spanning 1929 to present, with post-1973 data exhibiting optimal completeness.

4. Methods

Fig.2 illustrates the main procedures involved in the production of the Global Base Dataset-First Estimate Daily Data (GLBD-FED). The Integrated Surface Database (ISD) served as the data source, from which daily Tmax, Tave, and Tmin were derived using new methods after correcting for misrecorded data. All daily data underwent quality control and were assigned a quality code and date boundary code.

https://doi.org/10.5194/essd-2025-771
Preprint. Discussion started: 25 February 2026

Open Access Earth System Science Data Discussions

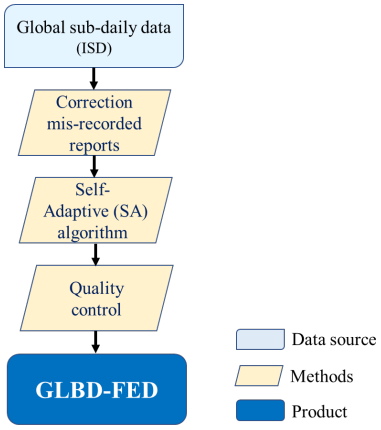

Figure 2 Main procedures of GLBD-FED production

4.1. Correction for Mis-recorded sub-daily Tmax/Tmin in data source

The quality of the data source is one of the most critical factors influencing the final data product. Notably, there were numerous misrecorded values for Tmax and Tmin over 12-hour and 24-hour periods in the global hourly data, particularly in South America.

Fig.3 presents a case study from San Antonio Oeste, Argentina (877840-99999), covering January 5 to January 12, 2023. The red and green lines represent the hourly upper limits of temperature derived from Tmax-12h and Tmax-24h, respectively, while the black circles indicate hourly Tave. Panel (a) displays results from the raw data, revealing that San Antonio Oeste tends to record Tmax-24h at 1200 UTC and Tmax-12h at 0000 and 1200 UTC. Although the hourly temperature upper limits derived from these records sometimes overlap, they differ significantly at other times. The green lines (derived from Tmax-24h) are consistently lower than the hourly Tave, suggesting that these Tmax-24h values are likely erroneous due to incorrect recording.

In this study, these data were not simply labeled with an ‘error’ quality code; efforts were made to restore them through the following procedures:

1. Tmax-24h records at hh:00 were compared with the highest hourly Tave from the previous 12 hours (Tave-12hhigh) and 24 hours (Tave-24hhigh). If Tmax-24h < Tave-

https://doi.org/10.5194/essd-2025-771
Preprint. Discussion started: 25 February 2026

24hhigh - 0.5°C and Tmax-24h ≥ Tave-12hhigh, it indicates that the Tmax-12h at hh:00 was incorrectly recorded as Tmax-24h and should be corrected.

2. Tmax-12h records at hh:00 were similarly compared with the highest hourly Tave from the previous 12 hours and 24 hours. If Tmax-12h > Tave-12hhigh + 0.5°C and Tmax-12h ≤ Tave-24hhigh, it suggests that the Tmax-24h at hh:00 was inaccurately recorded as Tmax-12h and should also be corrected.
3. The corrections for Tmin-24h and Tmin-12h followed a similar approach, but comparisons were made with the lowest hourly Tave from the previous 12 hours and 24 hours.

Fig.3 panel (b) displays the corrected results. The misrecorded Tmax-24h values were restored to Tmax-12h, and the derived hourly upper limit temperatures now align closely with the hourly Tave.

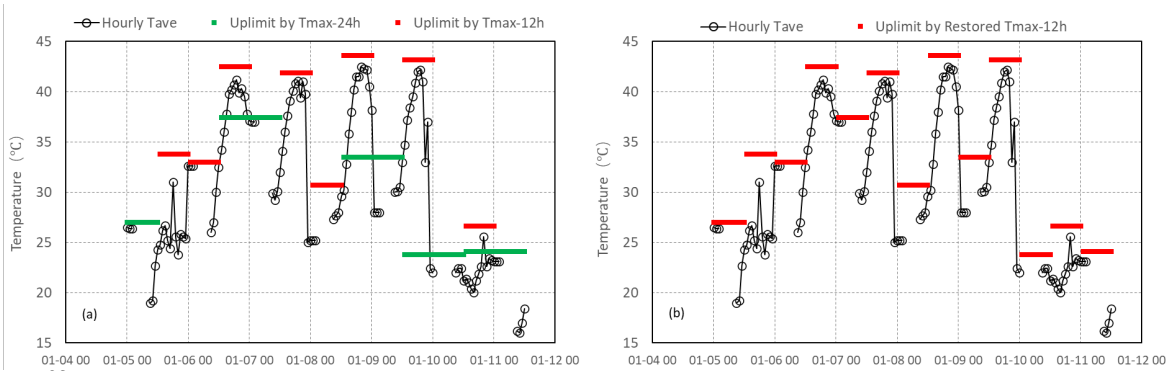

Figure 3 The hourly average temperature and the hourly up-limit of temperature derived from Tmax-12h/24h during 5th Jan to 12th Jan 2023 at San Antonio Oeste, Argentina. Panel a and b represent the results from raw and restored data, respectively. The red and green lines are hourly up limit of temperature derived from Tmax-12h and Tmax-24h, respectively, and the black cycles are hourly Tave.

4.2. New algorithms for in-situ daily temperature calculation

Aiming to obtain a set of global daily temperature data standing for the air temperature status under prospective dateline, new algorithms were developed.

https://doi.org/10.5194/essd-2025-771
Preprint. Discussion started: 25 February 2026

4.2.1. Dateline management for daily data calculation

The standardized and preferred dateline for calculating daily Tmax, Tave, and Tmin is set at 0000-2400 UTC. When standard 0000-2400 UTC calculations are unfeasible, a graduated adjustment protocol (±hh offsets in 1-hour increments, up to ±12 hours) is employed to maximize data retention while maintaining temporal consistency. All adjustments made are systematically recorded in the final metadata outputs, ensuring comprehensive data inclusion and maximal uniformity in dateline across the dataset.

4.2.2. Equidistant sampling for daily Tave calculation

As discussed in Section 3.1, deriving daily Tave from the average of four hourly Tave records at 6-hour intervals proves to be both effective and efficient. The daily average temperature is calculated as the following formulae

$$Tave^{1}_{daily} = (Tave_{hh} + Tave_{hh+6hours} + Tave_{hh+12hours} + Tave_{hh+18hours})/4 \quad (1)$$

$$hh = 0000, 0100, \ldots 0600\ UTC$$

In this context, Tave represents the average temperature, with the subscript "daily" indicating data for the day and "hh" denoting the hour. The value of hh ranges from 0000 to 0600 UTC.

4.2.3. Reaggregation for daily Tmax and Tmin calculation

Sub-daily Tmax and Tmin records were temporally decomposed into finer intervals, following the precipitation data processing protocols established by Yang et al. 2020. This approach facilitated probabilistic recombination into daily Tmax and Tmin values under prospective dateline. Fig.4 illustrates a case of daily Tmin calculation using the reaggregation algorithm at False Pass, US (700638-99999) on October 11, 2024. During the period from October 11 to October 12, False Pass recorded Tmin-12h at 1200 UTC and Tmin-24h at 0900 UTC. Initially, a less apparent Tmin-15h at 0000 UTC on October 12 (-1.7°C, indicated by the dashed deep green arrow) was derived from the Tmin-24h at 0900 UTC (4.4°C, light blue arrow) and Tmin-12h at 1200 UTC on October 12 (-1.7°C, deep blue arrow). This value was then combined with the Tmin-12h at 1200 UTC on October 11 (-1.1°C, light blue arrow) to produce the daily Tmin value for October 11 (-

https://doi.org/10.5194/essd-2025-771
Preprint. Discussion started: 25 February 2026

1.7°C), which was the minimum recorded during that day.

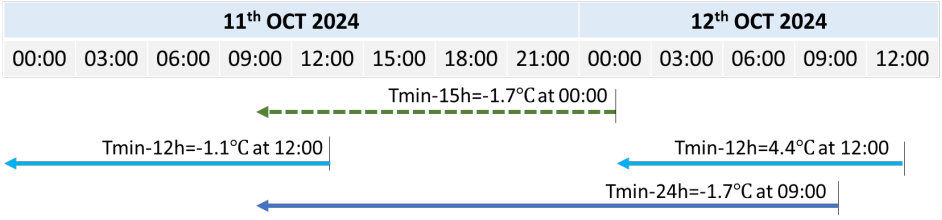

Figure 4 An application of reaggregation algorithm for daily Tmin value at False Pass, US (700638-99999) on 11th OCT 2024. The solid light and deep blue arrows are measured Tmin-12h and Tmin-24h, respectively; the dash light and deep green arrows are Tmin-12h and Tmin-15h concluded from the measured ones, respectively.

In comparison to the original method (which used either two consecutive Tmax/Tmin records over 12 hours or one Tmax/Tmin record over 24 hours), the reaggregation algorithm demonstrates a significant improvement in the production of daily Tmax and Tmin data. Fig.5 illustrates the average data volume of global daily Tmax and Tmin obtained by the two methods in 2023. The volume of daily Tmax data increased by 64%, rising from approximately 3,400 to 5,600 entries per day, while the volume of daily Tmin data grew by 45%, increasing from 4,100 to 5,900 entries per day.

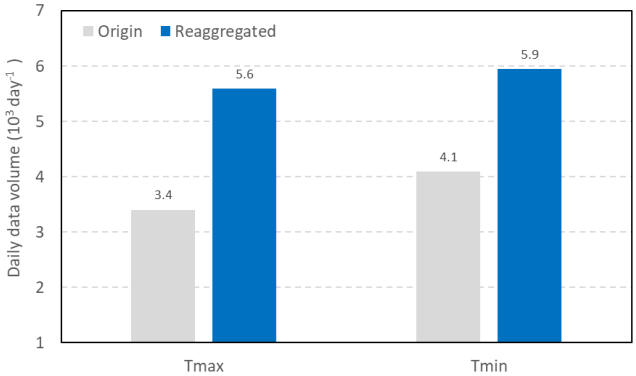

Figure 5 Average data volume of global daily Tmax and Tmin in 2023. The gray and blue bars represent the data calculated by origin and reaggregated methods, respectively.

Fig.6 illustrates the spatial distribution of the increased data generated by the SA algorithm. It is evident that the new algorithm enhances the global data volume, particularly over

https://doi.org/10.5194/essd-2025-771
Preprint. Discussion started: 25 February 2026

regions such as America, Australia, western Europe, and southern Asia. Tmax exhibits a more notable increase than Tmin, likely due to the scarcity of Tmax-12h and Tmax-24h records, particularly in Australia.

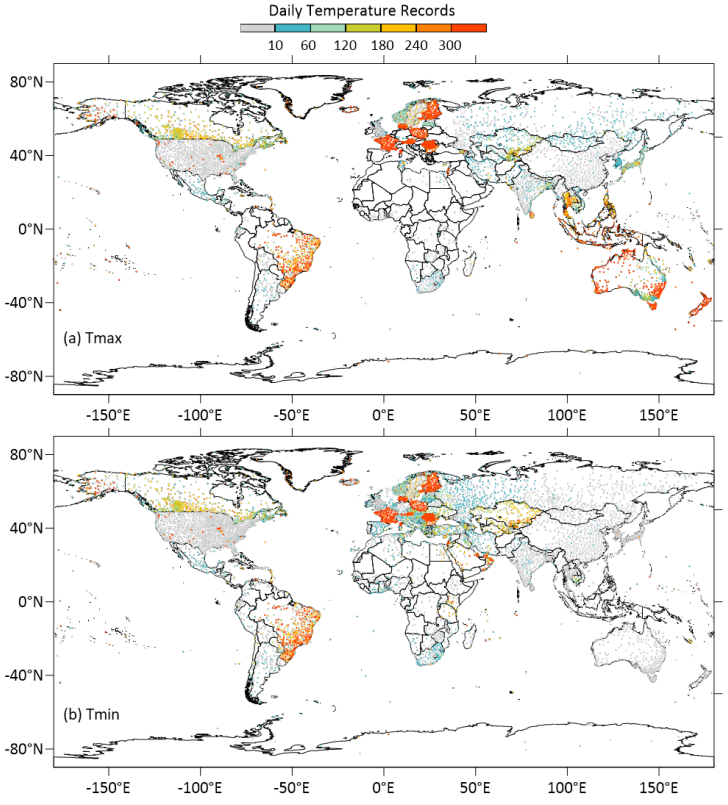

Figure 6 The spatial distribution of the increasing Tmax (panel a) and Tmin (panel b) data improved by reaggregated algorithm in 2023. The color represents increasing data volume.

Similar to GSOD, if the reaggregation algorithm fails, the maxima and minima records in hourly Tave serve as supplementary estimators for Tmax and Tmin, respectively, provided that there is at least 21 hours of temporal coverage.

4.3. Data quality controls

Quality controls were implemented for both the input hourly data and the produced daily

https://doi.org/10.5194/essd-2025-771
Preprint. Discussion started: 25 February 2026


Open Access Earth System Science Data Discussions

data. Global hourly temperature data quality tests include a spike value test, a stuck value test (which identifies prolonged sequences of the same value in the data series), and an inner consistency test (assessing the relationships between Tmax, Tave, and Tmin). The daily data underwent these same tests, along with additional temporal and spatial consistency tests. Details of these tests for daily data are provided in the Appendix.

Data quality results are flagged at each step and categorized into three groups: credible, suspicious, and erroneous. The quality test results at each stage are compiled into a final assessment of data quality levels. A final quality level is flagged as credible if there is no more than one suspicious test result and no erroneous test results. Conversely, a value is flagged as erroneous if more than one erroneous test result is found; otherwise, the final quality level is classified as suspicious.

5. Results

In this section, we first present the temporal changes and spatial coverage of the global in-situ daily temperature data volume of GLBD-FED. This is followed by comparisons of data values between GLBD-FED and GSOD, along with further discussions.

5.1. In-situ Data Volume and Spatial Coverage

Fig.7 presents the spatial distribution (panels a1, a2, and a3) and temporal changes (panels b1, b2, and b3) of global daily Tmax, Tave, and Tmin data from 1981 to 2024. The colorful dots in panel a indicate the duration of daily data at each site, while the gray and black curves represent the daily data volume and the 15-point smoothing results, respectively.

Tmax, Tave, and Tmin exhibit very similar spatial distributions and temporal changes over the last four decades. Panel a1, a2, and a3 show approximately 17,000 sites with at least one year of daily Tmax data. Sites in China, Japan, and central Europe have extensive time series of daily Tmax (≥40 years, indicated by red dots). Western Europe and the US

https://doi.org/10.5194/essd-2025-771
Preprint. Discussion started: 25 February 2026

demonstrate a high spatial density of daily Tmax data. Notably, inconsistencies in U.S. station metadata (e.g., station 72200654926 [43.617°N, 96.217°W] post-2005 vs. 72200699999 [43.621°N, 96.216°W] pre-2005) have resulted in many short time series (green and blue dots, <20 years of records). Brazil also displays a high spatial density of data, with most stations beginning temperature observations in the last decade. Substantial sites with at least 20 years of daily temperature data can be found in southern Canada, coastal Australia, Russia, and southern Asia. Although the Antarctic and Arctic regions are among the most challenging for meteorological observation globally, dozens of sites have commenced measurements in the current century.

The global daily data volume for Tmax, Tave, and Tmin has increased significantly over the last four decades. As shown in panels b1, b2, and b3, the global daily data volume rose from approximately 3,000 entries per day in the 1980s to around 10,000 entries per day in recent years.

https://doi.org/10.5194/essd-2025-771
Preprint. Discussion started: 25 February 2026

281

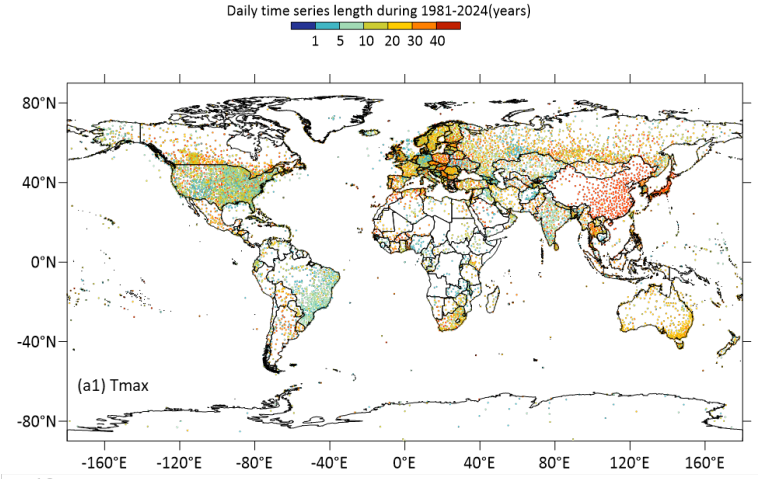

282

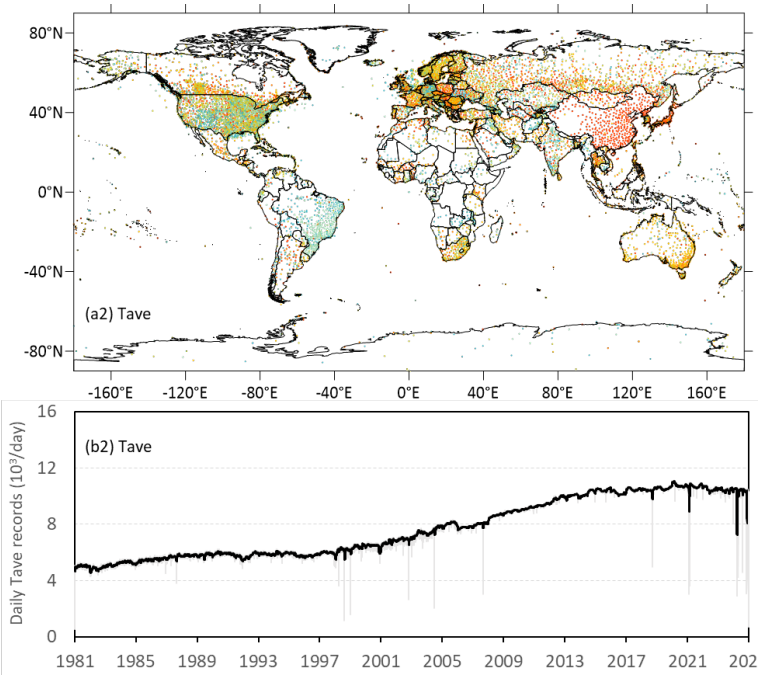

283

https://doi.org/10.5194/essd-2025-771
Preprint. Discussion started: 25 February 2026

Open Access Earth System Science Data Discussions

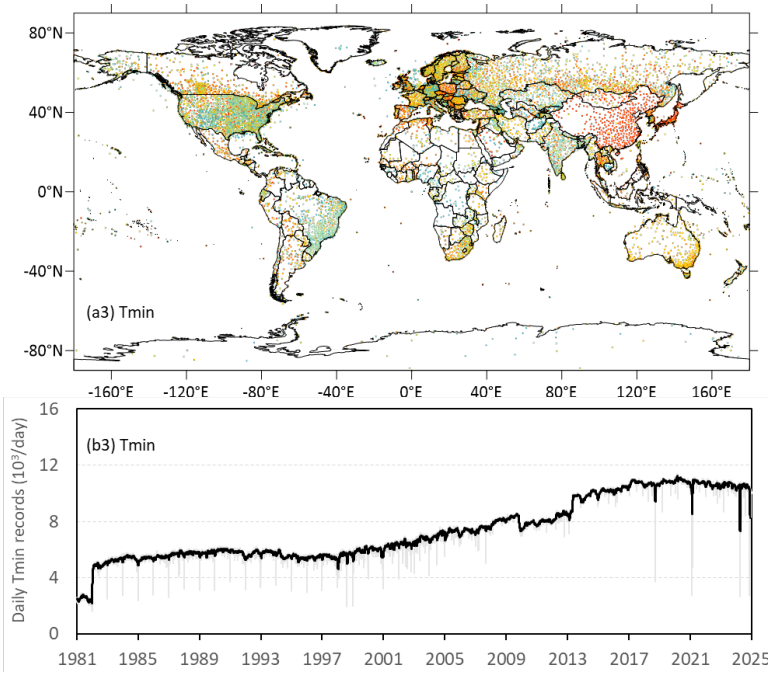

Figure 7 The spatial distribution (panel a1, a2, and a3) and temporal changes (panel b1, b2 and b3) of global daily temperature data during 1981-2024. Panel a1 and b1 represent the Tmax, panel a2 and b2 represent the Tave, panel c1 and c2 represent the Tmin. The colorful dots in panel a represent the length of the daily data at sites; the gray and black curves stand for the daily data volume and the 15 points-smoothing result, respectively.

https://doi.org/10.5194/essd-2025-771
Preprint. Discussion started: 25 February 2026

5.2. Comparison of daily temperature with GSOD

Fig.8 presents the multi-decadal time series (1981-2024) of global daily temperature differences between GSOD and GLBD-FED. Nearly all records of GLBD-FED shown in Fig.7 were comparted. It is clear that GSOD manifest warmer daily Tmax (around +0.3℃), colder Tmin (around -0.3℃) and nearly same daily Tave (around +0.1℃) relative to GLBD-FED in the whole period. That mean the research based on GSOD daily temperature data probably produce more remarkable climate extreme events than that based on GLBD-FED.

The difference in daily data definitions between GLBD-FED and GSOD is the primary cause of the systematic variability in Tmax and Tmin. GLBD-FED considers records that could or almost represent the highest or lowest temperature during the 24-hour period as daily Tmax and Tmin data, while GSOD selects the highest and lowest records within the 24 hours. This means that in GSOD, accumulated Tmax and Tmin records covering two days that represent the high or low values from the previous day (e.g., Tmax/Tmin-24h at 0300 UTC) may be treated as the daily Tmax and Tmin data for the following day if they are the highest or lowest values. The impact of this daily data definition is discussed in detail in Section 5.3.1.

https://doi.org/10.5194/essd-2025-771
Preprint. Discussion started: 25 February 2026

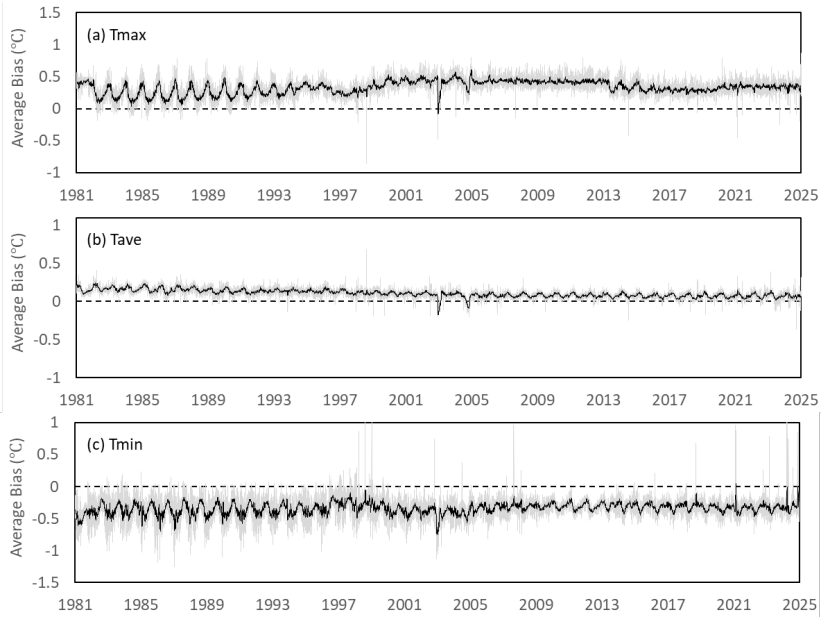

Figure 8 The daily time series of average difference in global in-situ daily temperature between GLBD-FED and GSOD (1981-2024) (GSOD minus GLBD-FED). The gray and black lines are the daily and 15 points-smoothing results, respectively. Panel (a), (b), and (c) stand for the results of Tmax, Tave and Tmin, respectively.

Fig.9 illustrates the spatiotemporal heterogeneity of daily temperature discrepancies between GSOD and GLBD-FED from 1981 to 2024. The sites in GSOD with higher daily Tmax (⩾0.5°C) relative to GLBD-FED are primarily located in Southern Africa, Brazil, Argentina, Canada, and the western United States (panel a1), accounting for 21.4% of all sites (approximately 17,000) (panel a2).

Interestingly, GSOD shows lower Tmax values in China compared to GLBD-FED. This discrepancy arises from several types of reports labeled with the same ID in the ISD. The Metar and Synoptic reports in China are independent and measured at different sites. Metar temperature reports tend to be lower than Synoptic temperature reports since the latter are mostly recorded in urban areas. GSOD prioritized Metar reports as data sources, while GLBD-FED optimized Synoptic reports, leading to the observed negative bias in

https://doi.org/10.5194/essd-2025-771
Preprint. Discussion started: 25 February 2026

China. This issue is discussed in more detail in Section 5.3.2.

Meanwhile, sites in GSOD with lower daily Tmin (≤-0.5°C) compared to GLBD-FED are predominantly found in Australia, Russia, and Northeast Asia (panel c1), representing 17.4% of all sites. Daily Tave from GSOD and GLBD-FED exhibits much greater consistency compared to Tmax and Tmin (panel b1), with 95.3% of sites maintaining differences within ±0.5°C (panel b2).

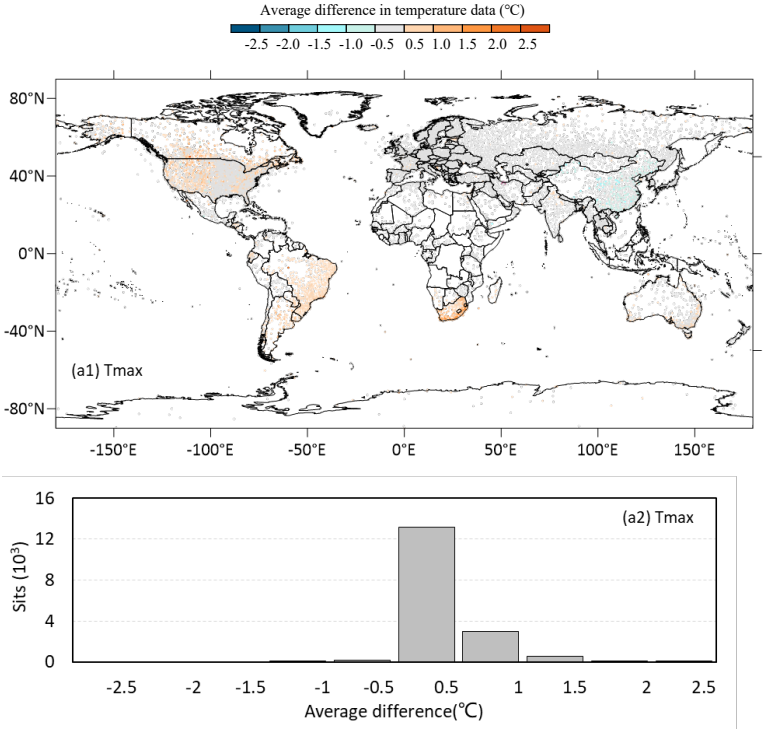

https://doi.org/10.5194/essd-2025-771
Preprint. Discussion started: 25 February 2026

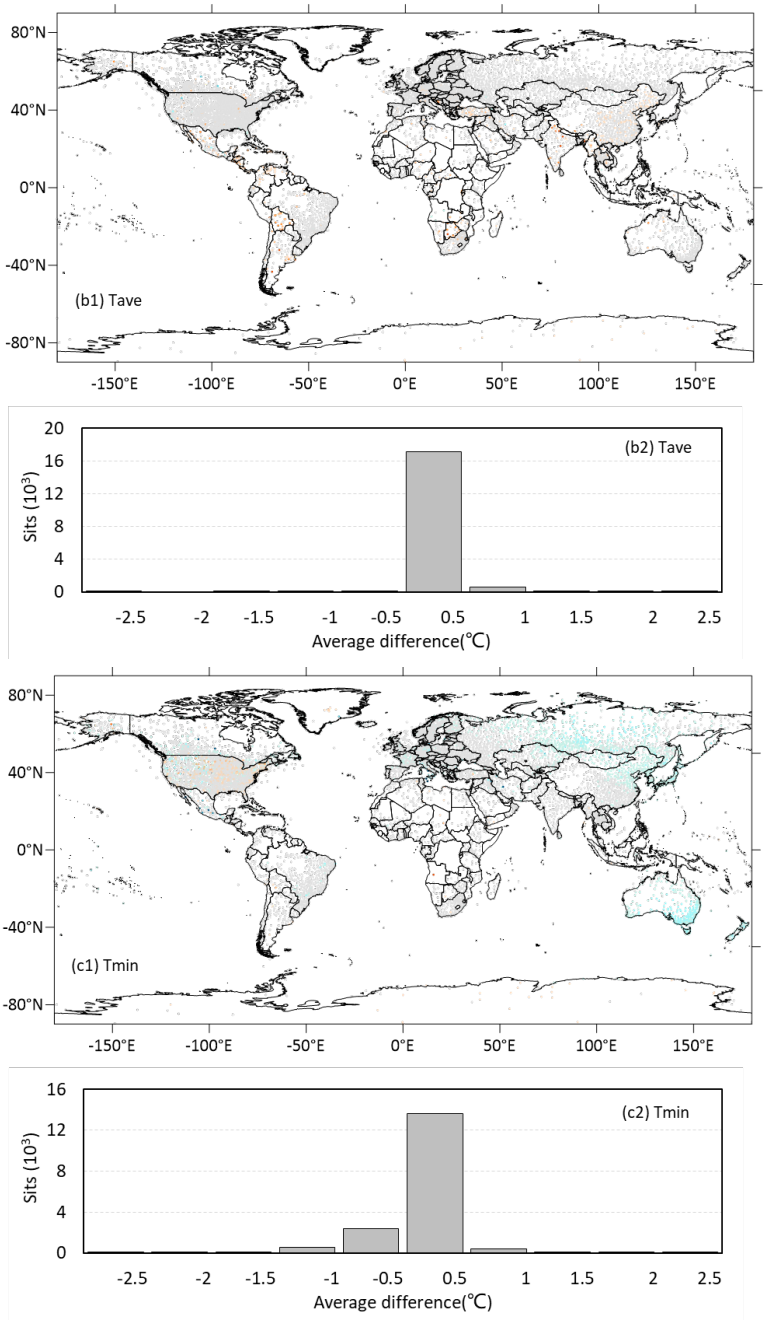

Figure 9 Spatial distribution of the difference in-situ daily temperature data between GLBD-FED and GSOD during 1981-2024 (GSOD minus GLBD-FED). Panel a1, b1, c1 show the difference in Tmax, Tave and Tmin at each site, respectively. Panel a2, b2, c2 represent the sites number distribution with diversities.

https://doi.org/10.5194/essd-2025-771
Preprint. Discussion started: 25 February 2026

5.3. The causes for the discrepancy in daily temperature data

GLBD-FED and GSOD employ different algorithms to produce daily temperature data, resulting in discrepancies in data properties and biases between the two datasets, particularly for Tmax and Tmin. Table 1 outlines three main differences in the key processes of daily Tmax and Tmin data production between GLBD-FED and GSOD.

First, GLBD-FED and GSOD have distinct definitions for daily Tmax and Tmin data. GLBD-FED considers records that could or almost represent the highest or lowest temperature in a 24-hour period as daily Tmax and Tmin, while GSOD selects the highest and lowest records within the 24 hours.

Second, although both GLBD-FED and GSOD utilize sub-daily data shared globally through the Global Telecommunication System (GTS) as their data source, they apply this data differently. GLBD-FED prefers Synoptic reports over Meteorological Aerodrome (Metar) and other reports when multiple types of sub-daily reports share the same ID, whereas GSOD does the opposite.

Third, GLBD-FED makes efforts to adjust the daily temperature boundary to 0000 UTC whenever possible, while GSOD retains the highest and lowest values as they appear within the 24-hour period.

Table 1 the comparison of the key processes in daily Tmax/Tmin calculation between GBLD-FED and GSOD

No	Key processes	GLBD-FED	GSOD
1	The definition of the daily Tmax/Tmin data	The records could/almost represent the highest/lowest temperature over the 24h.	The highest/lowest records in the 24h.
2	The preference about the data source as there are several types of sub-daily reports labeled by the same ID	Synoptic reports	Meteorological Aerodrome Reports

https://doi.org/10.5194/essd-2025-771
Preprint. Discussion started: 25 February 2026

Open Access Earth System Science Data Discussions

3	The date boundary for global daily data	Adjust the daily boundary of the daily temperature value to 00:00 UTC as much as possible.	/

366

367 **5.3.1. The influence of the daily data definition**

368 Fig.10 displays the variations in air temperature at the SINPO station (470460) in North
369 Korea from May 20 to May 23, 2014. The hollow black dots represent hourly average air
370 temperatures recorded at fixed observation times, while the red and yellow dots indicate
371 the Tmin-12h and Tmin-24h values recorded at 0000 and 2100 UTC, respectively. The
372 light blue curve in panel (a) and the dark blue curve in panel (b) denote the lower-bound
373 estimates of air temperature derived from the daily Tmin values based on GSOD and
374 GLBD-FED data, respectively.

375

376 In the GSOD dataset (panel a), the daily Tmin value for the SINPO station was recorded
377 as 10.6°C for four consecutive days. This occurred because the Tmin-24h recorded at 0000
378 UTC on May 21, which was the lowest value during the period from May 21 to May 22,
379 was treated as the daily Tmin for both May 21 and May 22. Similarly, the Tmin-24h
380 recorded at 0000 UTC on May 23 was adopted as the daily Tmin for both May 22 and
381 May 23. As a result, the derived daily Tmin values for May 21 and May 23 are evidently
382 underestimated and duplicated.

383

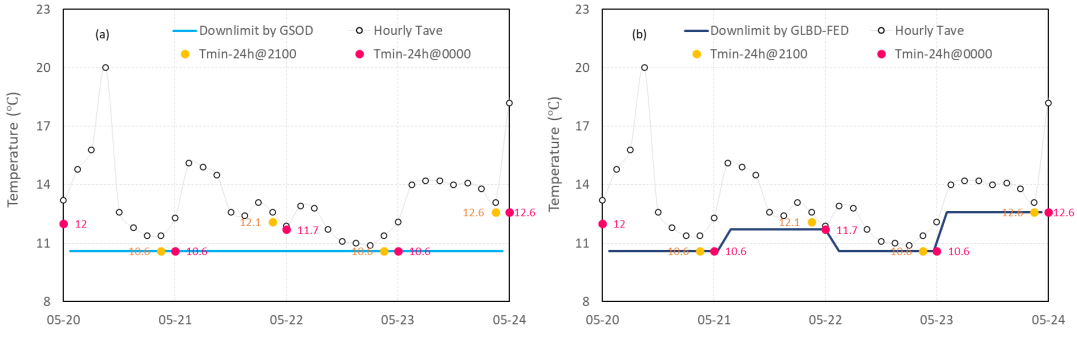

385 Figure 10 Variations in air temperature at the SINPO station (470460) in North Korea from May 20 to
386 May 23, 2014. The hollow black dots represent hourly average air temperatures recorded at fixed

https://doi.org/10.5194/essd-2025-771
Preprint. Discussion started: 25 February 2026

observation times, while the red and yellow dots indicate the Tmin-12h and Tmin-24h values recorded at 0000 and 2100UTC, respectively. The light blue curve in panel (a) and the dark blue curve in panel (b) denotes the lower-bound estimate of air temperature derived from the daily Tmin values based on GSOD and GLBD-FED data, respectively.

Fig.11 presents a comparison of daily Tmax values at the Plettenberg Bay station (689310). The abscissa and ordinate represent the daily values from the GLBD-FED and GSOD datasets, respectively. The red solid dots indicate data points that are repeated from previous values, while the black hollow dots represent non-repeating values. The mean difference between the two sets of daily Tmax values shown in the figure is 1.3°C, indicating that GSOD generally reports warmer temperatures compared to GLBD-FED.

The data points are further categorized into two groups based on the presence of consecutive identical values in GSOD: red points (repeated GSOD values) and black points (non-repeated GSOD values). Interestingly, approximately one-third of the Tmax daily values from GSOD this year were likely duplicated records, showing a significantly positive bias of about 3.2°C. Excluding these red points results in a roughly 70% reduction in the mean bias, decreasing it to 0.4°C. This suggests that GSOD's definition of daily Tmax and Tmin data may lead to repeated records, resulting in more extreme temperature results (higher Tmax and lower Tmin) compared to GLBD-FED.

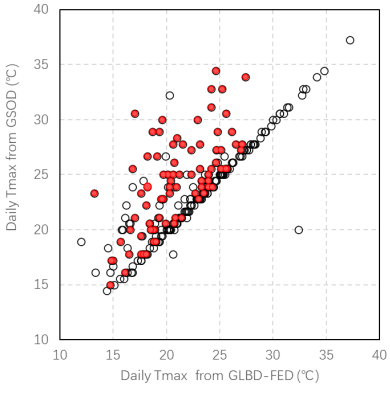

Figure 11 A comparison of daily Tmax values at the Plettenberg Bay station (689310), South Africa, for the year 2024. The abscissa and ordinate represent the daily values from the GLBD-FED and GSOD

https://doi.org/10.5194/essd-2025-771
Preprint. Discussion started: 25 February 2026

datasets, respectively. The red solid dots indicate the data that are repeated with their previous ones (86 points), while the black hollow dots represent non-repeating values (172 points).

5.3.2. The influence of the choice of data source

There are several types of sub-daily reports labeled with the same ID in the ISD, and these reports are not always measured at the same location. Both GLBD-FED and GSOD treat these reports independently based on their types, but they have different preferences. Given the more uniform observation mechanisms in meteorological stations compared to airports, GLBD-FED prioritizes synoptic reports over Metar reports as data sources.

Table 2 presents a case study for Ulan Bator, Mongolia, where two types of sub-daily reports labeled as 442920-99999 originate from different sites in the ISD. GSOD shows significantly lower daily Tmin values for Ulan Bator compared to GLBD-FED, which uses synoptic reports (Fig.12 panel a), with an average bias of -4.5°C. These values nearly overlap with the daily Tmin derived from Metar reports (Figure 12 panel b). This indicates that the daily Tmin data for Ulan Bator produced from sub-daily temperature reports at airports are much lower than those from meteorological sites. Thus, the choice of data source has a substantial impact on the data quality.

Table 2 Ulan Bator, Mongolia (442920-99999) sub-daily reports

Reports Type	Longitude	Latitude	Altitude
Synoptic Report (FM-12)	36.067°N	120.333°E	77m
Metar Report (FM-15)	36.266°N	120.374°E	10.05m

https://doi.org/10.5194/essd-2025-771
Preprint. Discussion started: 25 February 2026

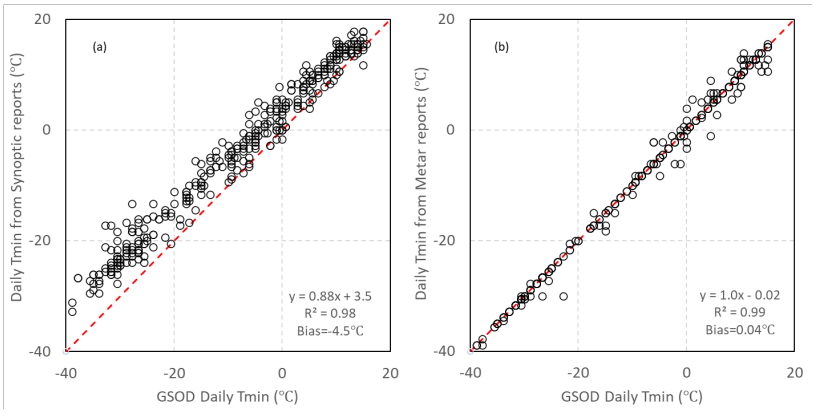

Figure 12 The comparison of daily Tmin at Ulan Bator, Mongolia (442920-99999) between GLBD-FED and GSOD in 2024. Panel a is the comparison between GLBD-FED (Synoptic reports) and GSOD data, while panel b is similar to panel a but with GLBD-FED (Metar reports).

5.3.3. The influence of the date boundary treatment

The systematic discrepancies identified in Fig.8 originate from methodological divergences between GLBD-FED and GSOD, specifically in temporal alignment frameworks. Fig.13 (a) illustrates this mechanism through a case study at Villa Reynolds, Argentina (31.96°S, 65.13°W), where GSOD exhibits a systematic Tmax warm bias of +1.6°C relative to GLBD-FED. This deviation occurs because GSOD attributes maximum temperatures to calendar days using the 1200 UTC Tmax-24h (0900 local time), in contrast to GLBD-FED's UTC-aligned approach, which reconstructs diurnal extremes by integrating next-day 1200 UTC observations with contemporaneous measurements. Temporal recalibration experiments (Fig.13 (b)) effectively mitigate this discrepancy, achieving inter-dataset convergence at 0.1°C with improved correlation (R^2=0.99 compared to the original R^2=0.87).

https://doi.org/10.5194/essd-2025-771
Preprint. Discussion started: 25 February 2026

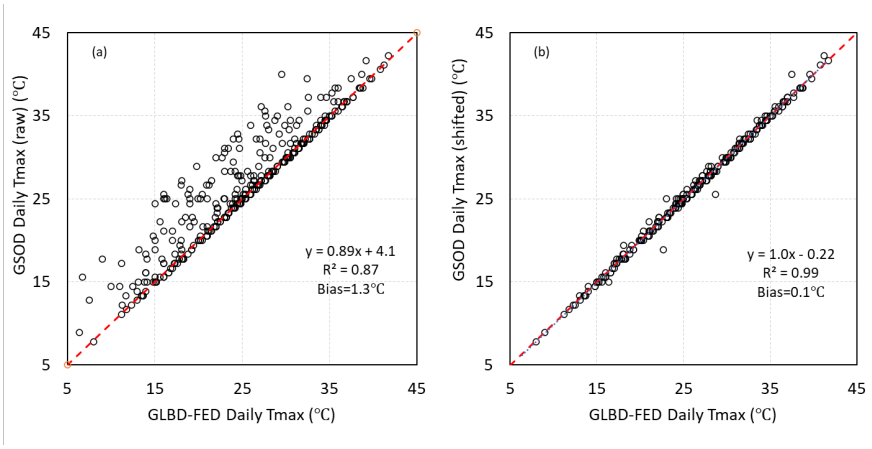

Figure 13 The comparison of daily Tmax at Villa Reynolds Argentina between GLBD-FED and GSOD in 2022. Panel a is the comparison between GLBD-FED and original GSOD data, while panel b is the comparison between GLBD-FED and date shifted (forward moving) GSOD data.

6. Data availability

The global in-situ temperature daily data are publicly available at https://zenodo.org/records/17895292

7. Conclusion

This study develops GLBD-FED, a global in situ daily temperature dataset encompassing maximum (Tmax), average (Tave), and minimum (Tmin) temperatures, constructed using quasi-real-time sub-daily observations from ISD. The main results of this study show that:

1. To produce a global daily dataset representing maximum, minimum, and average temperatures over a 24-hour period (i.e., one day), we developed a new algorithm that decomposes sub-daily Tmax and Tmin records into finer intervals and then reaggregates them into daily Tmax and Tmin under prospective dateline. Compared to the original method (which relied on two consecutive Tmax/Tmin records over 12 hours or one Tmax/Tmin record over 24 hours), the new method increased daily Tmax and Tmin by 64% and 45%, respectively. A correction for misrecorded Tmax and Tmin records was also implemented.

https://doi.org/10.5194/essd-2025-771
Preprint. Discussion started: 25 February 2026

2. GLBD-FED includes Tmax, Tave, and Tmin data from approximately 17,000 global sites covering the period from 1981 to 2024. The daily temperature volume of GLBD-FED increased from 3,000 records per day in the 1980s to 10,000 records per day in the 2020s. America and Asia show high spatial densities of daily temperature data, especially in recent years. In comparison to GSOD, Tmax and Tmin from GLBD-FED exhibit more temperate performance, with slightly lower daily Tmax (approximately -0.3°C) and higher daily Tmin (approximately +0.3°C), resulting in nearly the same daily Tave (around +0.1°C). These differences are primarily attributed to the diversity in daily data definitions and the choice of data sources.

8. Author contributions

SY designed and carried out the study, performed the analyses, and drafted the manuscript. PMZ and XBZ contributed to the development of the manuscript framework, provided scientific guidance throughout the research process, and critically reviewed and revised the manuscript. ZJZ reviewed and edited the paper.

9. Competing interests

The contact authors have declared that none of the authors has any competing interests.

10. Acknowledgements

This work is supported by the National Natural Science Foundation of China (42475152) and The Joint Research Project for Meteorological Capacity Improvement (24NLTSZ005).

11. Appendix: Formulae used for Daily Data Quality

Data Quality Tests

Spike test

$$\mathrm{qc} = \begin{cases} credible, x_{lowerlimit} \le x_i \le x_{upperlimit} \\ wrong, x_i \ge x_{upperlimit} \ \ or \ x_i \le x_{lowerlimit} \end{cases}$$

https://doi.org/10.5194/essd-2025-771
Preprint. Discussion started: 25 February 2026

Open Access Earth System Science Data Discussions

$$x_{upperlimit} = \min[\max(\bar{x}) + 5℃, 80℃]$$

$$x_{lowerlimit} = \max[\min(\bar{x}) - 5℃, -80℃]$$

Where the subscript i stands for the measurement on the i-th day; $x_{upperlimit}$ /$x_{lowerlimit}$ is the upper/lower threshold value for the record and is the smaller/higher value between $\max(\bar{x}) + 5℃$ and 80℃, where $\bar{x}$ represents the subset of the historic measurements in the month (Jan, Feb,…Dec) which removes the smallest and largest 1% of values.

Inner consistency test

$$qc = \begin{Bmatrix} credible, Tmax \geq Tave \geq Tmin, \\ wrong, Tmax \leq Tave \leq Tmin \\ doubtful, else \end{Bmatrix}$$

Where the Tmax, Tave, Tmin stand for the daily Tmax, Tave, Tmin data, respectively

Temporal consistency test

$$qc = \begin{Bmatrix} credible, x_i \leq \mu + 2.5\sigma \\ wrong, x_i > \mu + 5\sigma \\ doubtful, \mu + 2.5\sigma < x_i \leq \mu + 5\sigma \end{Bmatrix}$$

$$\mu = \text{median}(\bar{x})$$

$$\sigma = \text{std}(\bar{x})$$

Where the μ and σ are the median value and standard deviation of $\bar{x}$, respectively.

Spatial consistency test

$$qc = \begin{Bmatrix} credible, \delta_i \leq \min[\bar{\delta} + 2.5\nabla\delta, 10℃] \\ doubtful, \min[\bar{\delta} + 2.5\nabla\delta, 10℃] < \delta_i < \min[\bar{\delta} + 3.5\nabla\delta, 15℃] \\ wrong, \delta_i \geq \min[\bar{\delta} + 3.5\nabla\delta, 15℃] \end{Bmatrix}$$

$$\delta_i = \sqrt{\frac{\sum_{j=1}^{m}(x_j - x_i)^2}{m}}$$

$$\bar{\delta} = median(\delta_i)$$

$$\nabla\delta = \text{std}(\delta_i)$$

Where the subscript j stands for the j-th neighbouring sites (within the 100km radius around the candidate site) and m is the total number of neighbouring sites.

https://doi.org/10.5194/essd-2025-771
Preprint. Discussion started: 25 February 2026

Stuck values test

$$qc = \begin{Bmatrix} wrong, \sigma = 0 \\ credible, else \end{Bmatrix}$$

$$\sigma = \mathrm{std}(x_{i-1}, x_i, x_{i+1})$$

$$\mu = \mathrm{mean}(x_{i-1}, x_i, x_{i+1})$$

where σ and μ are the standard deviation and smoothing average of 3 days measurements, respectively.

12. Reference

Adler RF, Huffman GJ, Chang A, Ferraro R, Xie P, Janowiak J, Rudolf B, Schneider U, Curtis S, Bolvin D, Gruber A, Susskind J, A. P., 2003: The Version 2 Global Precipitation Climatology Project (GPCP) Monthly Precipitation Analysis (1979-Present). *J. Hydrometeor*, 4, 1147–1167.

Beck, H. E., A. I. J. M. Van Dijk, V. Levizzani, J. Schellekens, D. G. Miralles, B. Martens, and A. De Roo, 2017: MSWEP: 3-hourly 0.25° global gridded precipitation (1979-2015) by merging gauge, satellite, and reanalysis data. *Hydrol Earth Syst Sci*, 21, 589–615, https://doi.org/10.5194/hess-21-589-2017.

——, E. F. Wood, M. Pan, C. K. Fisher, D. G. Miralles, A. I. J. M. Van Dijk, T. R. McVicar, and R. F. Adler, 2019: MSWep v2 Global 3-hourly 0.1° precipitation: Methodology and quantitative assessment. *Bull Am Meteorol Soc*, 100, 473–500, https://doi.org/10.1175/BAMS-D-17-0138.1.

Blenkinsop, S., and Coauthors, 2018: The INTENSE project : using observations and models to understand the past , present and future of sub-daily rainfall extremes. *Advances in Science & Research*, 15, 117–126.

Daly, C., 2002: Variable influence of terrain on precipitation patterns: Deliniation and use of effective terrain height in PRISM. *Prism*, 1–7, https://doi.org/10.1007/s10329-011-0282-2.

Dietzsch, F., A. Andersson, M. Ziese, M. Schröder, K. Raykova, K. Schamm, and A. Becker, 2017: A Global ETCCDI-Based Precipitation Climatology from Satellite and

https://doi.org/10.5194/essd-2025-771
Preprint. Discussion started: 25 February 2026

Rain Gauge Measurements. *Climate*, 5, 9, https://doi.org/10.3390/cli5010009.

Harris, I., P. D. Jones, T. J. Osborn, and D. H. Lister, 2014: Updated high-resolution grids of monthly climatic observations - the CRU TS3.10 Dataset. *International Journal of Climatology*, 34, 623–642, https://doi.org/10.1002/joc.3711.

Harris, I., T. J. Osborn, P. Jones, and D. Lister, 2020: Version 4 of the CRU TS monthly high-resolution gridded multivariate climate dataset. *Scientific Data 2020 7:1*, 7, 1–18, https://doi.org/10.1038/s41597-020-0453-3.

Hulme, M., 1991: An intercomparison of model and observed global precipitation climatologies. *Geophy. Res. Lett*, 18, 1715–1718.

Hulme, M., 1992: A 1951-80 global land precipitation climatology for the evaluation of general Circulation Models. *Climate. Dyn.*, 7, 57–72, https://doi.org/10.1007/BF00209609.

Janowiak, J. E., A. Gruber, C. R. Kondragunta, R. E. Livezey, and G. J. Huffman, 1998: A Comparison of the NCEP-NCAR Reanalysis Precipitation and the GPCP Rain Gauge-Satellite Combined Dataset with Observational Error Considerations. *J Clim*, 11, 2960–2979.

Jones, P. D., and M. Hulme, 1996: Calculating regional climatic time series for temperature and precipitation: methods and illustrations. *International Journal of Climatology*, 16, 361–377, https://doi.org/10.1002/(SICI)1097-0088(199604)16:4<361::AID-JOC53>3.0.CO;2-F.

——, and a. Moberg, 2003: Hemispheric and large-scale surface air temperature variations: An extensive revision and an update to 2001. *J Clim*, 16, 206–223, https://doi.org/10.1175/1520-0442(2003)016<0206:HALSSA>2.0.CO;2.

Kamiguchi, K., O. Arakawa, A. Kitoh, A. Yatagai, A. Hamada, and N. Yasutomi, 2010: Development of APHRO_JP, the first Japanese high-resolution daily precipitation product for more than 100 years. *Hydrological Research Letters*, 4, 60–64, https://doi.org/10.3178/hrl.4.60.

Klein Tank, A. M. G., and Coauthors, 2002: Daily dataset of 20th-century surface air

https://doi.org/10.5194/essd-2025-771
Preprint. Discussion started: 25 February 2026

579 temperature and precipitation series for the European Climate Assessment.
580 *International Journal of Climatology*, 22, 1441–1453,
581 https://doi.org/10.1002/joc.773.
582 Menne, M. J., I. Durre, R. S. Vose, B. E. Gleason, and T. G. Houston, 2012: An overview
583 of the global historical climatology network-daily database. *J Atmos Ocean Technol*,
584 29, 897–910, https://doi.org/10.1175/JTECH-D-11-00103.1.
585 Mitchell, T. D., and P. D. Jones, 2005: An improved method of constructing a database of
586 monthly climate observations and associated high-resolution grids. *International*
587 *Journal of Climatology*, 25, 693–712, https://doi.org/10.1002/joc.1181.
588 NCEI, 2017: Global Surface Summary of the Day.
589 New, M., M. Hulme, and P. Jones, 1999: Representing Twentieth-Century Space – Time
590 Climate Variability . Part I : Development of a 1961 – 90 Mean Monthly Terrestrial
591 Climatology. *J Clim*, 12, 829–856, https://doi.org/10.1175/1520-
592 0442(1999)012<0829:RTCSTC>2.0.CO;2.
593 New, M., M. Hulme, and P. Jones, 2000: Representing twentieth-century space-time
594 climate variability. Part II: Development of 1901-96 monthly grids of terrestrial
595 surface climate. *J Clim*, 13, 2217–2238, https://doi.org/10.1175/1520-
596 0442(2000)013<2217:RTCSTC>2.0.CO;2.
597 Rudolf, B., 1993: Management and analysis of precipit at ion dat a on a routine basis.
598 *International Symposium on Precipitat ion and Evaporation*, 20–24.
599 Schamm, K., M. Ziese, A. Becker, P. Finger, A. Meyer-Christoffer, U. Schneider, M.
600 Schröder, and P. Stender, 2014: Global gridded precipitation over land: A description
601 of the new GPCC First Guess Daily product. *Earth Syst Sci Data*, 6, 49–60,
602 https://doi.org/10.5194/essd-6-49-2014.
603 Schneider, U., 1993: *The GPCC quality control system for gauge measured precipitation*
604 *data*. WMO.
605 ——, A. Becker, M. Ziese, and B. Rudolf, 2018: Global Precipitation Analysis Products
606 of the GPCC. *Global Precipitation Climatology Centre (GPCC)*, 1–14.

https://doi.org/10.5194/essd-2025-771
Preprint. Discussion started: 25 February 2026

607 Smith, A., N. Lott, and R. Vose, 2011: The integrated surface database: Recent
608 developments and partnerships. *Bull Am Meteorol Soc*, 92, 704–708,
609 https://doi.org/10.1175/2011BAMS3015.1.
610 Su Yang, Panmao Zhai, Xuebin Zhang, and Zijiang Zhou.: Development of a global in-
611 situ daily temperature dataset preferentially for 0000–2400 UTC from 1981–
612 2024, ZENODO [data set], https://doi.org/10.5281/zenodo.17895292, 2025.
613 Westra1, S., and Coauthors, 2014: Future changes to the intensity and frequency of short-
614 duration extreme rainfall. *Reviews of Geophysics*, 52, 522–555,
615 https://doi.org/10.1002/2014RG000464.Received.
616 WMO, 2015: *Manual on Codes - International Codes*. 2011th ed. 466pp.
617 Xie, P., M. Chen, Y. Fukushima, S. Yang, C. Liu, A. Yatagai, and T. Hayasaka, 2007: A
618 Gauge-Based Analysis of Daily Precipitation over East Asia. *J Hydrometeorol*, 8,
619 607–626, https://doi.org/10.1175/JHM583.1.
620 Yang, S., P. D. Jones, H. Jiang, and Z. Zhou, 2020: Development of a near-real-time global
621 in situ daily precipitation dataset for 0000–0000 UTC. *International Journal of*
622 *Climatology*, 40, 2795–2810, https://doi.org/10.1002/JOC.6367.
623 Yatagai, A., K. Kamiguchi, O. Arakawa, A. Hamada, N. Yasutomi, and A. Kitoh, 2012:
624 Aphrodite constructing a long-term daily gridded precipitation dataset for Asia based
625 on a dense network of rain gauges. *Bull Am Meteorol Soc*, 93, 1401–1415,
626 https://doi.org/10.1175/BAMS-D-11-00122.1.
627
628
629
630
631